Detailed Depositional Resolutions in Miocene Sands of HT-3X Well, Hai Thach Field, Nam Con Son Basin, Vietnam

Quan Vo Thi Hai

Abstract— Nam Con Son sedimentary basin is one of the very important oil and gas basins in offshore Vietnam. Hai Thach field of block 05-2 contains mostly gas accumulations in fine-grained, sand/mud-rich turbidite system, which was deposited in a turbidite channel and fan environment. Major Upper Miocene reservoir of HT-3X lies above a well-developed unconformity. The main objectives of this study are to reconstruct depositional environment and to assess the reservoir quality using data from 14 meters of core samples and digital wireline data of the well HT-3X.

The wireline log and core data shown that the vertical sequences of representative facies of the well mainly range from Tb to Te divisions of Bouma sequences with predominance of Tb and Tc compared to Td and Te divisions. Sediments in this well were deposited in a submarine fan association with very fine to fine-grained, homogeneous sandstones that have high porosity and permeability, indicating good quality of reservoir. Sediments are comprised mainly of the following sedimentary structures: massive, laminated sandstones, convoluted bedding, laminated ripples, cross-laminated ripples, deformed sandstones, contorted bedding. Very fine to fine-grained, mud/sand-rich sediments were the result of relatively high-density turbidity currents with longer transport route from the sediment source to the basin and a resulting better separate of sand and mud.

Index Terms— Core description, Facies, Hai Thach field, Miocene sands, Nam Con Son basin, Turbidite, Wireline log.

1 Introduction

THE Hai Thach field lies in block 05-2 of the Nam Con Son basin, offshore Southern Vietnam, approximately 290 km South-East of Vung Tau city (Fig. 1). This field is about 35 km North-East of the Nam Con Son pipeline and the water depth from 130 m to 145 m. This was discovered in 1995 with HT-1X well, appraised in 1996 by HT-2X well.

The HT-2X was drilled to test the extent of Upper Miocene clastic reservoirs and deepened to evaluate Middle/Lower Miocene clastics on the eastern flank of Hai Thach Horst. HT-3X well was also drilled as the second appraisal in the block 05.2 [1].

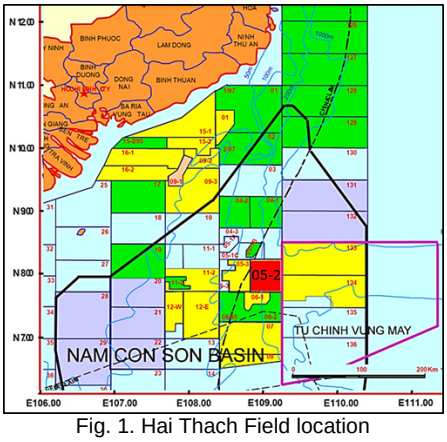

Fig. 1. Hai Thach Field location

- Quan Vo Thi Hai is currently working at Analysis Laboratory Center, Vietnam Petroleum Institute, Block E2b-5, Sai Gon Hi-Tech Park, District 9, Ho Chi Minh city, Vietnam. E-mail: quanvth@vpi.pvn.vn

2 Geological Framework

2.1 Stratigraphy of Hai Thach Field

Wells in Hai Thach field arc drilled through Upper to Lower Miocene sediments, therefore, biostratigraphic study is carried out only to this stratigraphic level (Fig. 2). Stratigraphy of regional well, including the Hai Thach well, identified by biostratigraphic data and tie to seismic horizon is as follows:

Upper Miocene to recent (Bien Dong-Nam Con Son Formations): As the result of Nannofossil analysis the key seismic horizons within the Upper Miocene can be identified from seabed down to seismic Green horizon. Jade horizon is well correlated among wells in blocks 05.2 and 05.3, between nannofossil zones and is the base of shelf progradation. No intervals of condensed or missing section observed. A sand and silty mud level was encountered in the HT-2X well and was deposited in deep water environment.

Middle Miocene (Thong-Mang Cau Formation): Below the Middle Miocene unconformity, the Hai Thach field is faulted and divided into Hai Thach Horst and Flanks (Fig. 2). The well results show that Middle Miocene lithology in the horst differs very much from those of the eastern flank.

The Middle Miocene stratigraphy within the HT-2X is predominantly open marine, outer shelf to bathyal which is in marked contrast to the shallow marine environments of the Middle Miocene on the horst and to the South. It is clear from this evidence that the faults around Hai Thach were very active in the Middle Miocene. The biostratigraphic analysis concentrated on trying to define the relationship between the

Middle Miocene sediments between these wells.

Lower Miocene (Dua Formation): The stratigraphy of the Lower Miocene is relatively poorly constrained compared to the overlying Middle and Upper Miocene. Nannofossils were relatively uncommon, and many of those recovered showed evidence of reworking. Similarily useful marine microfaunal axa were also relatively uncommon, reflecting the increasing proximality of the depositional environment of the Lower Miocene.

east.

There is a significant variation in the age of faulting of different faults, along strike of some individual faults. The NE-SW trending faults to the NW and SE of Hai Thach appear to part of the same linked fault system during the Terracotta to orange period. It appears that there is also a system of later faults, like the main N-S trending western fault on Hai Thach, which cut the Middle Miocene unconformity. A simplified geological evolution of Hai Thach can be described as follows:

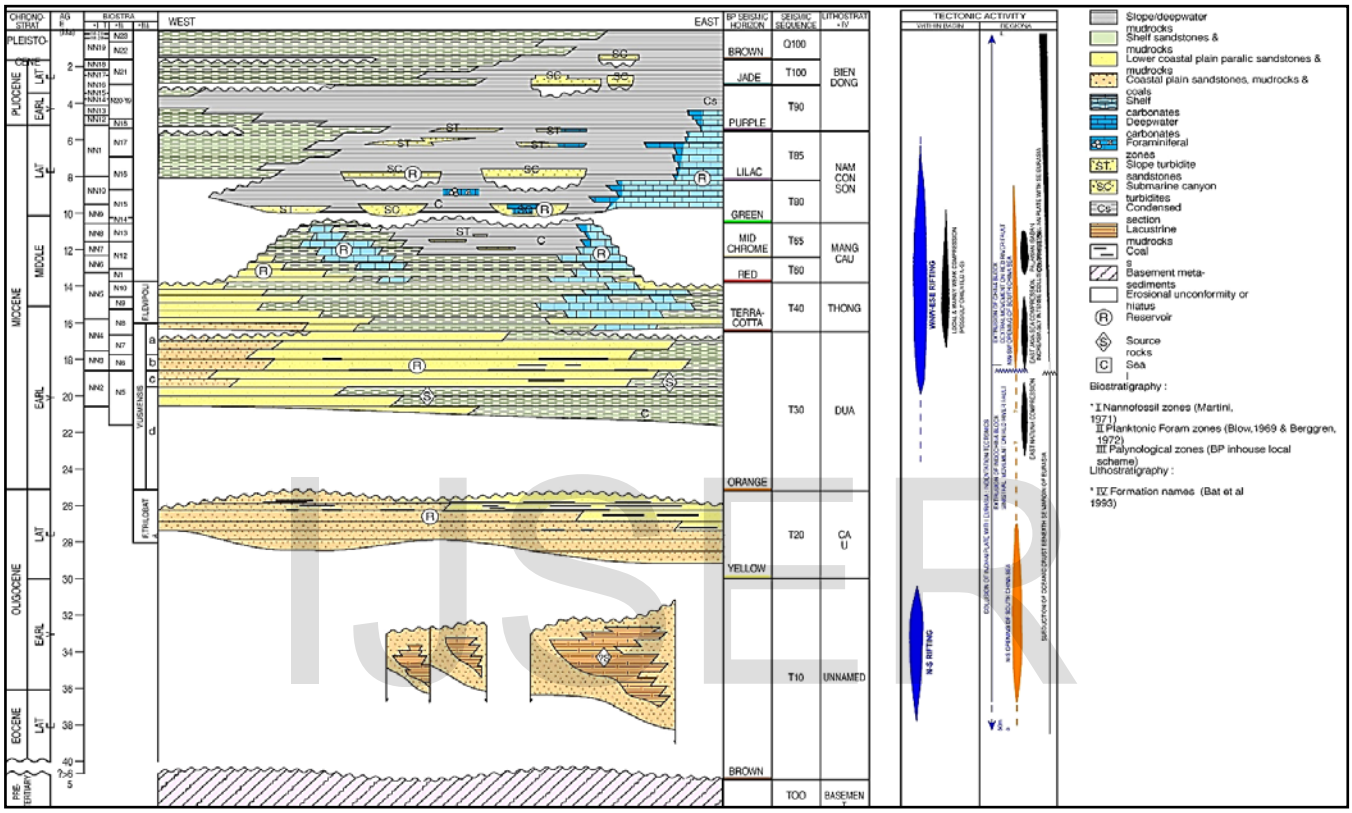

Fig. 2. Nam Con Son basin chronostratigraphic section

2.2 Structure and Basin Evolution

There are two major sequence stratigraphic elements controlling the distribution of facies within the Nam Con Son basin. The first is Upper Miocene-Recent post-rift and the second is related to Middle-Lower Miocene syn-rift. The post-rift is almost unaffected by faults and characterized in seismic by a parallel continuous sequence, overlaid by a prograding sequence (Fig. 3). The syn-rift is strongly affected by normal faults. Reservoirs within the horst indicate a general dipping from West to East and from South to North. The Northeast-Southwest fault system fragmented the Hai Thach into Hai Thach horst, bounded by two main bounding faults and two Hai Thach Flanks. The western flank is more subsided along a straight fault plane, while the eastern flank is rotated along a listic fault with a series of smaller faults stepping down to the

Oligocene: The Oligocene has not been penetrated in the Hai Thach field. As the basin is interpreted to be filled by locally derived fluvial/alluvial fan sediments with the possible presence of lacustrine facies in the central part, the mentioned facies could be present in Hai Thach deeper section.

Lower Miocene: Marine transgression with sands, silts, muds and occasionally carbonates deposited in marginal marine to shallow shelf environments.

Middle Miocene: Middle Miocene rifting terminated at the Green event, followed by thermal subsidence. Passive continental margin has been established with progradation from west to east within a highstand system tract. Turbidite sands have been formed at some levels within the bottom set areas of prograding wedges [1].

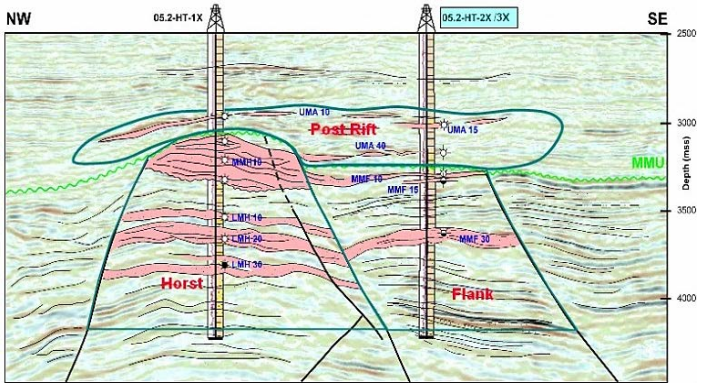

Fig. 3. Hai Thach schemetic cross section

3 Data and Methods

The data used in this study were provided by BP Exploration Ltd. (Vietnam) that consist of good conventional core #1 from 3286.01 to 3301.70 m and wireline logs.

This study focuses on the depositional environments and reservoir quality of the Upper Miocene of one well from the Hai Thach Field. Thus, the characteristics and quality of the lithofacies need to be understood by integrating core and wireline log data. Core gives useful information about biological, physical, and chemical characteristics such as grain size, biota, trace fossil, nodules, mottles of carbonate cement, visual porosity, fractures, layers and bedding contacts [2]. Wireline log provides petrophysical information. Combining both data sets gives very good information about depositional setting and reservoir characteristics. The well was interpreted using a deterministic method for shale volume, porosity, water saturation and permeability. Porosities were derived from the environmentally-corrected density, for oil and water sands, and combined with density and neutron tools, for gas sands. These methods are described in detail as follows:

Step 1: Lithofacies identification

GR cut off and cross plots versus density, sonic, resistivity and neutron porosity were used for determining lithofacies, especially uranium and MSFL cut off values have been used to distinguish carbonate cement. Variations in sedimentary structures, grain size, color, degree of bioturbations, bedding surfaces were observed in core. Thus, combining both wireline logs and core will give good results in lithofacies identification.

Step 2: Facies and depositional environment assessment

The whole length of the core was laid out and the following features were noted and recorded on the log: thickness, lithology, grain size and sedimentary structures. Core gamma ray was measured to integrate with wireline logs. Routine core plug measurements (porosity, permeability and grain density) were integrated by tying the plug data to their depths.

Combining lithology, sedimentary structures, grain size, biostratigraphy, etc. observed in core with wireline log shape are good indicators of lithology, facies and depositional environment. Some significant features pointed out as follows: (1) Sanding-upward and shaling-upward, blocky shape, funnel shape, bell shape and changes of thickness in separate units can be defined on conventional log responses; (2) Fining upward (FU), Coarsening upward (CU), sedimentary structures; (3) Structures and degree of bioturbation easily observed in core intervals. Therefore, in non-core intervals, they will be defined by combining log shape and corresponding features of cored sections

Step 3: Reservoir characterisation assessment

Core plug measurements were used to identify reservoir characteristics that correspond with each lithofacies by constructing separate histograms. Petrophysical was used to review and to study minerals and diagenesis that control reservoir properties. The core porosity-effective porosity relationship and the core porosity-permeability relationship were constructed to calculate reservoir properties in non-cored intervals for both wells.

In addition, a newly designed mini-permeameter probe was used for in situ measurements of permeability. The average volume of the probe is highly localized and is amenable to determining small-scale permeability variations [3]. The probe is also useful for measuring permeability with a sample spacing of 0.5 cm. Although this instrument gives lower accurate measurements than that of an automatic permeameter, these measurements were used with gas permeability values because they are variable consistent with gas permeability measurements, with the exception that those of less than 10 mD are unreliable. The formula used to calculate K from mini-permeameter measurements as in (1):

$$T = -0.8206 * \log_{10} K + 12.8737 \quad (1)$$

Where: T - mini-permeameter measurement
K - permeability (mD)

There is a good correlation between laboratory core permeabilities and mini-permeameter permiabilities in the 10-7500 mD range. The mini-permeameter estimates permeability in smaller rock volume (approximately 1 cm^3) than laboratory measurement (approximately 60 cm^3), thus they reflect the permeability variation over a core plug.

4 Core Description

Core photos show three main lithofacies including sandstone, interbedded shaly sandstone and mudstone that they are subdivided into smaller units for more detail based on sedimentary structures, degree of bioturbation and variation in grain size. These units are defined as massive sandstone/structureless/homogeneous (Ss), laminated sandstone (Sl), deformed sandstone (Sd) including disturbed, convoluted and contorted beddings, ripple cross-laminated sandstone, laminated shaly sand (Hsl), bioturbated shaly sand (Hsb), carbonaceous sandstone (Scc), mudstone (Ms) and bioturbated mudstone (Mb).

Massive/homogeneous sandstone (Ss): sandstone in this section is olive grey to light olive grey color, very fine- to fine-grained, well-sorted with no bioturbation and few or no sedimentary structures (Fig. 6d).

Laminated sandstone (Sl): olive grey color and very fine- to fine-grained with thinly bedded sandstones are sometimes found in core (Fig. 4c).

Deformed sandstone (Sd): deformed sandstone/soft-sediment deformation structure herein is found in the cores with olive to light olive grey color, very fine- to fine-grained, well-sorted sandstones. (Figs. 4c, 4d; 5a, 5b; 6b, 6d; 7a).

Laminated shaly sand (Hsl): this lithofacies consists of very fine- to fine-grained sand laminae interlayered with thin brown or dark grey shale beds, ranging from mm to cm scale (Figs. 4a, 5b, 6a, 6b, 7b). The degree of bioturbation is normally moderate. This is dominantly found in the cores and includes cross-laminated bedding and ripples.

Bioturbated shaly sand (Hsb): sediments of this lithofacies are very light grey to olive grey, fine-grained sandstone with a high shale content. Moderate bioturbation is found only at 3296 m (Fig. 6c).

Carbonate-cemented sandstone (Scc): the cement can be recognized by its hardness compared to the surrounding rock and bright mottles of carbonate with very light grey colour in fine-grained sandstone (Figs. 6a, 6c). This comprises stacked sandstone beds that are sometimes interbedded with carbonaceous mudstone layers. Several centimetres the cements are found in the interval 3288.40-3293.15 m.

Mudstone (Ms): this lithofacies is medium light grey to medium grey structureless mudstone with no bioturbation.

Bioturbated mudstone (Mb): this is characterized by a medium light grey mudstone with very low sandstone content and heavy bioturbation which has destroyed most primary sedimentary structures. Moderate to heavy bioturbated mudstone was observed at 3292.45 m and 3300.06 m (Figs. 5d, 7c).

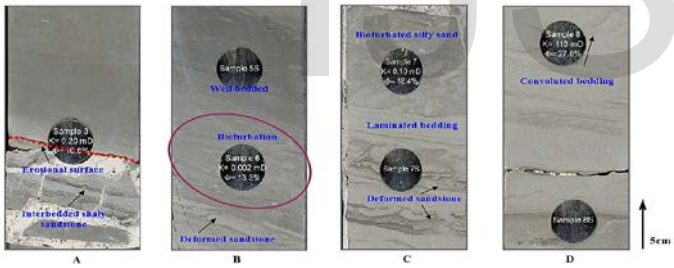

Fig. 4. Core description from 3286.90 m to 3288.60 m
(a) 3286.90 m (Hsl): medium light grey interbedded shaly sand, about several cm thickness with erosion surface at top; (b) 3287.30-3287.75 m (Ml & Mb): dark olive grey mudstone, well bedded, heavy bioturbation; (Sd): light olive grey sandstone, deformed sandstone; (c) 3288.06-3288.31 m (Sb & Sl): very light to olive grey, very fine to fine grained Sst, bioturbation silty sand, deformed sandstone; (Sd): structure, laminated bedding and deformed sandstone in cm scale; (d) 3288.34-3288.60 m (Sc): very light grey, fine grained sandstone, heavy carbonate cement

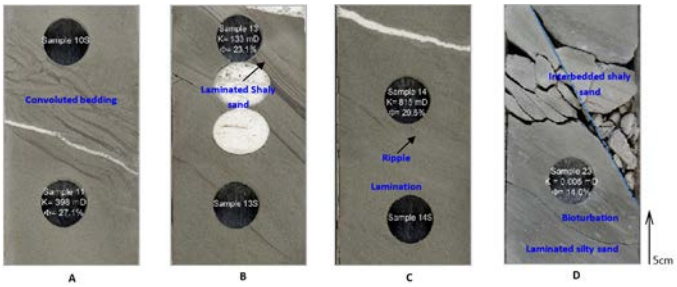

Fig. 5. Core description from 3288.17 m to 3292.45 m
(a) 3288.17 m (Sd): very light olive grey sandstone, very fine grains, convoluted bedding; (b) 3289.05 m (Hsl): light olive grey, very fine to fine grained sandstone with laminated shaly sand; (c) 3289.35 m (Sd): light olive grey, very fine to fine grained sandstone, ripple lamina; (d) 3292.45 m (Hsl, Mb, Sl): light olive grey interbedded shaly sand at top, heavy bioturbation and laminated silty sand at bottom.

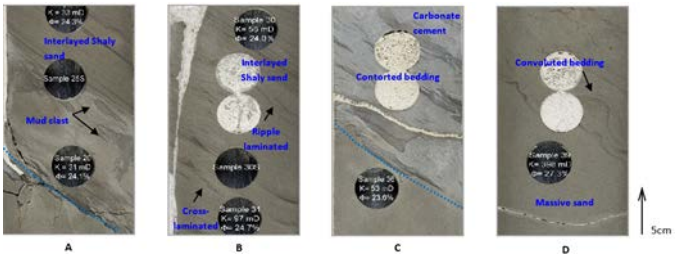

Fig. 6. Core description from 3293.15 m to 3297.10 m
(a) 3293.15 m (Hsl): light olive grey, very fine to fine grained sandstone with interbedded shaly sand, mud clasts, carbonate cement; (b) 3294.50-3294.80 m (Hsl, Sd): light olive grey to olive grey, very fine to fine grained sandstone with interbedded shaly sand at top, ripple and cross-laminated at bottom; (c) 3296.10 m (Sd): olive grey to very light olive grey, fine grained sandstone, contorted bedding, heavy carbonate cement; (d) 3297.10 m (Sd): olive grey, very fine to fine grained sandstone, convoluted bedding, massive sand

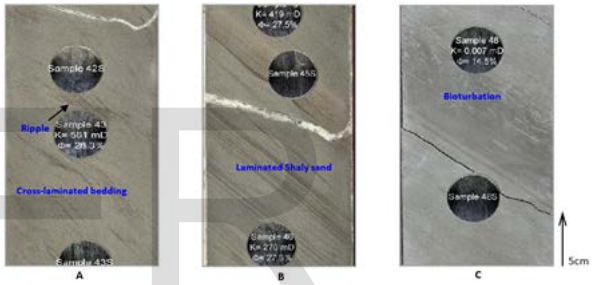

Fig. 7. Core description from 3298.35 m to 3300.06 m
(a) 3298.35 m (Sd): olive grey, very fine to fine grained sandstone with ripple and cross-laminated bedding; (b) 3299.27 m (Hsl): olive grey, interbedded shaly sand; (c) 3300.06 m (Mb): medium light grey mudstone, moderate bioturbation

5 Wireline Lithologies

Core depths were matched to the log depth by correlation between core porosity and wireline density-derived porosity. Once this was done, the core data were depth matched to the wireline gamma ray. Figs. 8 and 9 show mismatches and good matches of core gamma ray and wireline gamma ray and a good match of core porosity and wireline density-derived porosity. Figs 10a and 10b show the mismatch of core GR to the wireline GR and the core porosity to wireline porosity before depth matching. Details of the depth shift are shown in table 1.

TABLE 1
Depth Shift

Core depth (m)				Wireline depth (m)	
Core No.	Top	Base	Shift	Top	Base
2	3286.01	3287.22	+1.829	3287.84	3289.05
3, 4	3287.68	3301.70	+2.438	3290.12	3304.14

A well defined about 1.9 m mudstone bed separates the upper sand in upper and lower divisions. This bed recorded in

the depth from 3293.6 to 3295.5 m. Three major lithofacies were defined by the gamma ray cut-off values, sandstone (Ss), interbedded shaly sand (Hs) and mudstone (Ms). The lithofacies were mainly defined by cross plots of gamma ray and bulk density, bulk density and neutron (Figs. 11a, 11b) and sonic and gamma (Fig. 12a). Resistivity was also used for lithofacies identification where formation water was the same in the examined intervals. Sandstones have the highest resistivity values (Fig. 12b).

Generally, wireline lithofacies reveals a good correlation to core lithofacies, exception of intervals 3007-3008 m (log depth) and 3007.46-3008.46 m (core depth) do not match, this may be the vertical resolution of GR about 20-30 cm and thus can only be visually recognised in the core at a very small scales (mm).

A good match between wireline lithofacies recorded from the gamma ray and sonic log cross plot and core lithofacies. This result can be applied for reliable wireline lithofacies extrapolation in uncored intervals.

Litholofacies can be defined on density-derived effective porosity. Three layers can be seen with a fining upward trend that is consistent with changes in lithofacies using the GR cut-off, core porosity and core permeability (Fig. 13). The average values of the main log responses extracted from the various cross plots with corresponding lithofacies are shown in table 2.

TABLE 2
PARAMETERS TAKEN FROM WIRELINE CROSS PLOTS

Litho-facies	Code	GR (API)	RHOB (g/cc)	NPHI (v/v)	LLD (Ωm)	DT (µs/ft)
Sandstone	Ss	<83	2.06-2.43	0.25-0.30	2.49-30.21	98-118
Siltstone	Hs	81-92	2.12-2.43	0.31-0.35	2.45-13.69	100-111
Mudstone	Ms	>92	2.25-2.46	0.32-0.41	1.66-26.85	105-113

GR-gamma ray, RHOB-density, NPHI-neutron porosity, LLD-resistivity, DT-sonic

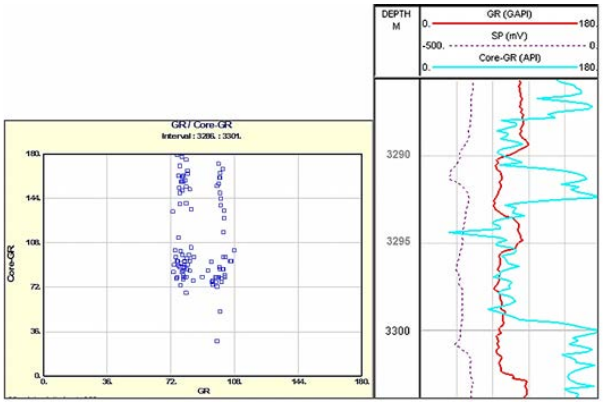

Fig. 8. Mismatch between core GR and wireline GR before depth shifting in 3286-3301 m

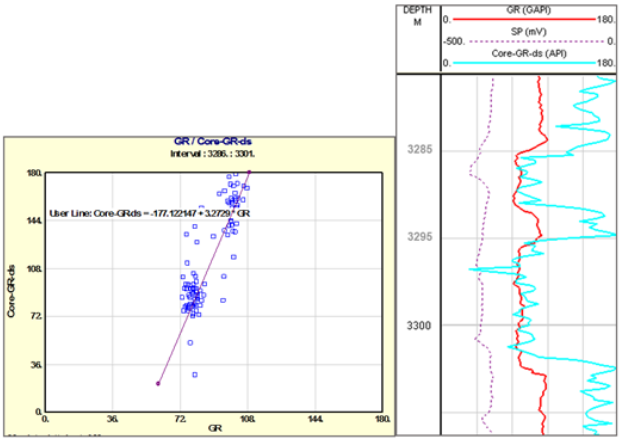

Fig. 9. Good match between core GR and wireline GR after depth shifting in 3286-3301 m

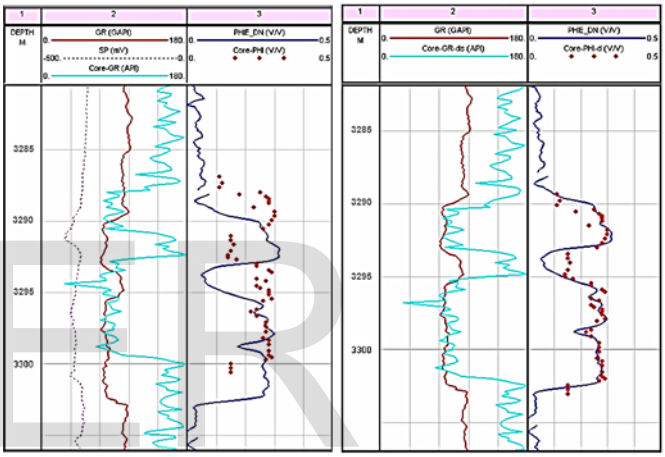

Fig. 10. (a) Mismatch of core and wireline data; (b) Good match of core and wireline data in 3286-3301 m

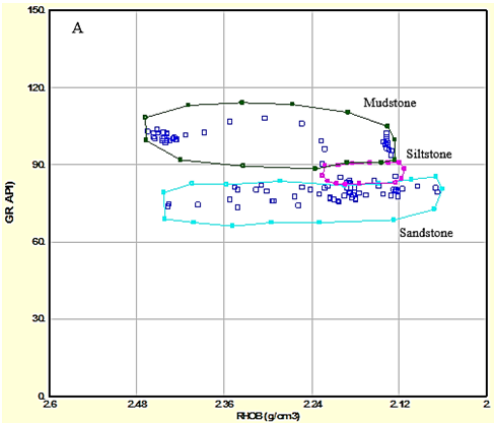

Fig. 11. (a) Density vs GR in 3286-3301 m

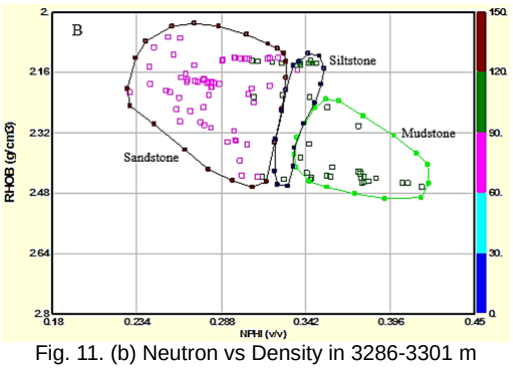

Fig. 11. (b) Neutron vs Density in 3286-3301 m

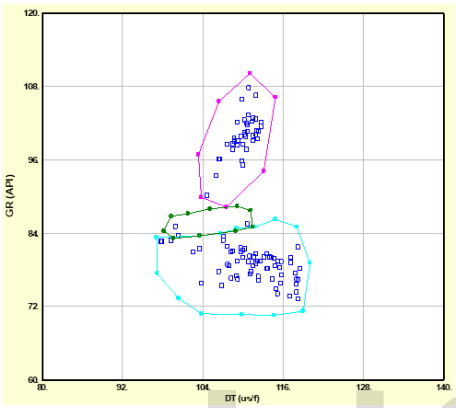

Fig. 12. (a) GR vs Sonic in 3286-3301 m

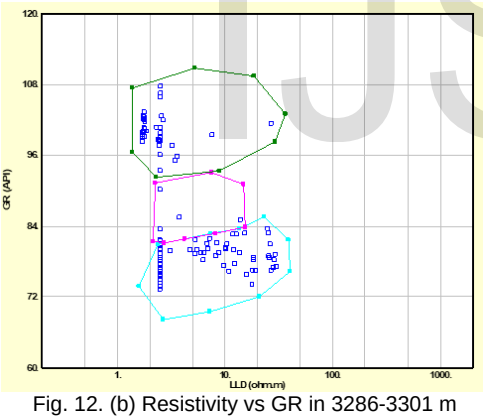

Fig. 12. (b) Resistivity vs GR in 3286-3301 m

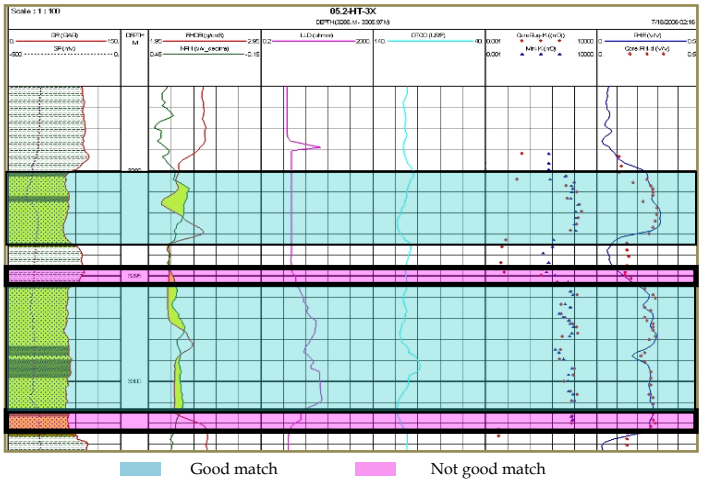

Fig. 13. GR cut off using Density and Neutron shows a good match

6 Facies Development And Depositional Environment

From wireline logs: A variety of vertical GR log profiles are developed with blocky sand common and minor presences of shaling-upward (bell shape) and sanding-upward, this seemingly homogeneous that is commonly an indicator of submarine association.

From core description: Core description identified a variety of facies, including the dominant very fine to fine-grained, moderately well-sorted sandstones. Grain size does not change much in most cored intervals. They are generally fine-grained sandstone with minor fining-upwards (FU) that is indicative of an upward decrease in grain size and upward increase in shale content; minor coaserning-upwards (CU) known as upward decrease in shale content.

The sedimentological log over the cored interval shows a very good match between the wireline facies and core interpretation. The vertical succession consists of upper sandstone and lower sandstone separated by 1.9 m mudstone bed.

6.1 Interval 3291-3300 m

The bottom of this section consists of about 1.5 m thick mudstone, indicative of deposition in low energy environment.

After that sea level rose and slowly increased in energy so sediments passed into Tb unit where interlayed laminated silty sand at 3299-3299.7 m. Rippled and convoluted sand comprise the overlying Tc unit at 3297-3298 m. Sea level changed and increased again with rapid sedimentation in high energy formed major massive sand at 3294.9-3296.3 m. Amalgamation surfaces and angular to subangular fractures commonly divide beds internally into subunits. The subunits thickness and lengths vary due to discontinuous nature of the amalgamation contacts (Fig. 4a). A few of siltstone beds have disrupted/convoluted bedding and outsized mud-clasts that are found in several intervals (Fig. 6a). The sandstones or sometimes interbedded siltstones are typically ripple laminated on a very fine scale with occasional horizontal laminations and/or cross-laminated bedding (Figs. 4c, 5b.) and convoluted bedding at 3297.10m (Fig. 6d). These indicate that sediments were deposited in a lower energy of environment.

Light grey color, very hard surface beds at 3296-3296.15 m contain a very low clay content because of heavy carbonate-cemented sandstone that common in marine mudstone tend to be more resistant to weathering than the bioturbated sandstone (Fig. 6c). Several intervals show weak carbonate-cemented sandstone such as 3293 m, 3298 m and 3299 m.

6.2 Interval 3286-3290 m

Very light olive grey to olive grey, very fine to fine-grained, moderately well-sorted, massive sandstone at 3289-3290 m with minor laminated ripples, subparallel lamination bedding at top indicate that the sediments were deposited in high energy environment. Very light olive grey to olive grey, coarse grade silt with very fine-grained sandstone found at the top of

the next Tb-Td Bouma divisions with the predominance of some structures observed in about 3m thick, light olive grey, very fine- to fin-grained sandstone as follows: deformed sandstone, load casts, convoluted beddings, ripples, laminated shaly sand (Figs. 4, 5). Burrows found again with moderate contribution vertical and horizontal intervals. Therefore, internal sedimentary structures are not apparent within most of the burrow sand, probably because of destruction by burrowing. Rare mud clasts are present in around 3288.70 m. Besides, carbonate cement is also discovered by bright spots/mottles on the sample with moderate content at around 3289.1 m.

Overlying these sands was about 1.5 m thick, medium grey to light grey mudstone with some visible bedding, burrows and abundant forams. This interval is defined as Te division.

These sands are relatively clean and were deposited in large basins on passive margins by sediments with a long terrestrial transport distances, areas a broad shelf and are delta sourced. These sandstones beds comprise of 5 to 9 m thick that alternate thick- to thin-bedded shale/siltstones according to Bouma divisions. In stratigraphically ascending order there are: thick-bedded sandstone, thin-bedded sandtone and siltstone, siltstone and mudstone. The variations in sedimentary structures and thickness indicate physical similarity between sandstones within the thick- and thin bedded intervals implies that they were deposited in by similar flow mechanisms. Their primary massive appearance with occasional water escapes features is consistent with rapid deposition by high density turbidite currents. The upper section changes from thick-bedded to thin-bedded sandstone, siltstone within basin-floor cycle could reflect autocyclic lobe switching between central lobe and distal lobe positions, or it could reflect changing flow density caused by cyclic changes in relative base level [4].

The abundance of laminated ripple or cross-laminated sandstones in this section shows that they are deposited within the slope fan turbidite beds which are attributed to the rapid dumping of sediment at the base of slope, both within scoured channels and in overbank settings. Conversely, most of the basin floor fan sandstones beds are primarily massive sand. It is conceivable that graded turbidites are present in distal fan intervals with low energy of current containing fine- to very fine-grained sandstones. Overall, the sandstone bodies of this well deposited in middle fan where starts or near the base of slope is a constructional or aggradational part of the fan and is dominated by a channel levee complex that dominate the depostional style in the distal region of the system (Fig. 14).

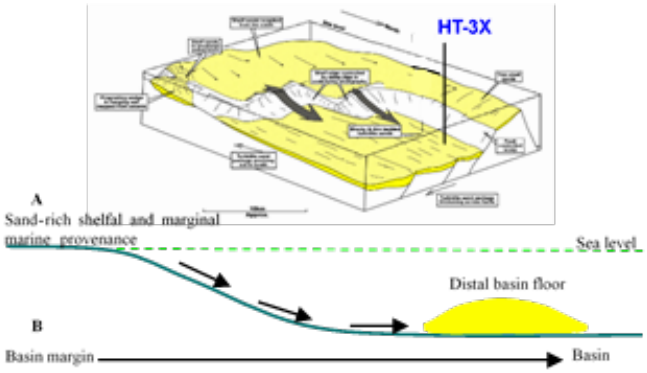

Fig. 14. Summary diagram illustrating the deposition within HT-3X

7 Reservoir Characterisation

The quality of a reservoir is defined by its hydrocarbon storage capacity and deliverability. The hydrocarbon storage capacity is characterized by the effective porosity and the size of reservoir, whereas the deliverability is a function of the permeability [5]. Thus, this part will focus on reservoir quality in term of porosity and permeability that relate to grain size, detrital clay, sedimentary structures, rock texture and controls on reservoir quality. Petrophysical, core and petrography data will be used for these purposes.

7.1 Reservoir quality

Reservoir quality and hydrocarbon production normally are assessed by routine core analysis that includes grain density, plug porosity and permeability.

Grain density measured for different lithofacies will be analyzed by using its histograms that show different lithofacies will give different ranges of density. Cores of this well mainly contain massive/laminated/deformed sandstones, interlayed shaly sand with much sedimentary structures recorded. Thus, the grain density values of these sandstones (2.66-2.68 g/cm^3) are lower than that of bioturbated shaly sand, bioturbated mudstone and mudstone. While mudstone has highest grain density values 2.74-2.75 g/cm^3, bioturbated shaly sand values ranging from 2.67-2.75 g/cm^3 (Fig. 15).

As the results, grain density values of bioturbated lithofacies are relatively higher that of laminated lithofacies. This is due to more detrital clay dispersed in the bioturbated than that of laminated lithofacies.

Generally, the average grain density of sandstones calculated for cored intervals is 2.67g/cm^3. This value will be applied for sand matrix to calculate wireline porosity. Total and effective porosity were calculated primarily using the density log and switched to a hydrocarbon-corrected density-neutron cross-plot method in gas zones [6]. Effective porosity was determined from shale correction of the total porosity. Core porosity, which is often higher than effective porosity, ties to total porosity as mentioned above. Values of core porosity mainly range from 27 to 30%. Depending on qualitative assessment of porosity and permeability, most of lithofacies have porosity values of more than 15% giving a very good

quality, with exception of mudstone with porosity values of less than 15%, indicating poor to fair quality.

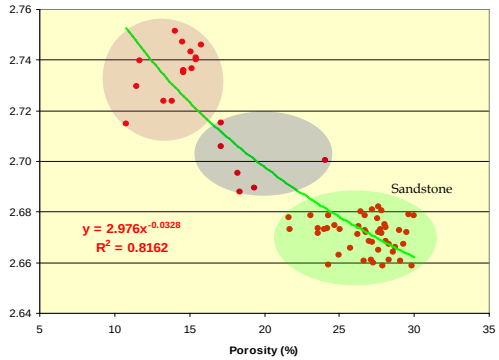

Fig. 15. Grain density vs porosity

Permeability values of different lithofacies in cored intervals show that the laminated/massive, deformed sandstones are of fair to good permeability (104-1045mD). Bioturbated shaly sand and bioturbated mudstone facies are poor to fair and moderate in permeability ranges (Fig. 16). Given the absence of core data, permeability has been determined using a porosity-permeability cross-plot based on overburden corrected core data taken from different lithofacies.

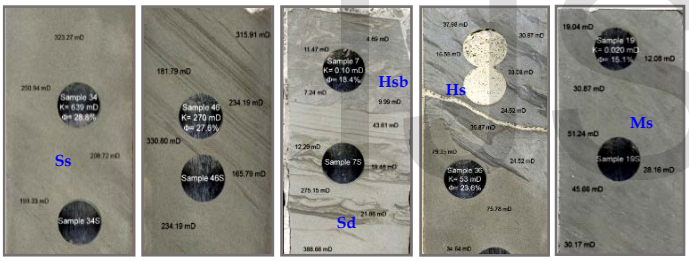

Fig. 16. An example of permeability in different lithofacies
(a) Massive sandstone (Ss); (b) Laminated shaly sand (Hsl); (c) Bioturbated shaly sand (Hsb), deformed sandstone (Sd); (d) Contorted bedding/mud clast/shaly sand with high carbonate cement; (e) Mudstone (Ms)

The major factors controlling sandstone permeability are grain size, sorting, compaction and cementation. Using this approach, the porosity-permeability trends that result from the progressive application of various diagenetic processes can be understood.

Moreover, to construct a reservoir property predicting model for the uncored interval based on plug data, the relationships between porosity and permeability were calculated for various lithofacies (Fig. 17).

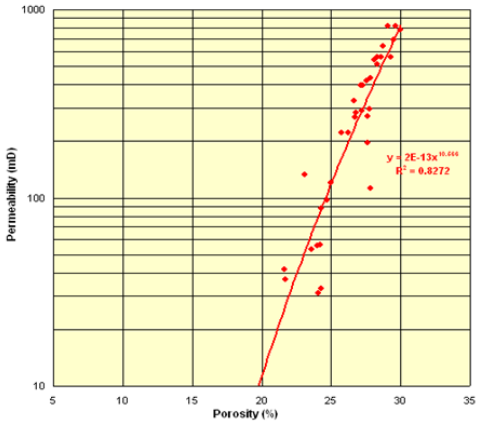

Fig. 17. Porosity and Permeability in the depth from 3286 to 3301 m

Porosity and Permeability relationship

The major factors controlling sandstone permeability are grain size, sorting, compaction and cementation. Using this approach, the porosity-permeability trends that result from the progressive application of various diagenetic processes can be understood.

Moreover, to construct a reservoir property predicting model for the uncored interval based on plug data, the relationships between porosity and permeability were calculated for various lithofacies. The porosity-permeability relationship shows a very good correlation coefficient in (2):

$R^2=0.8272$ with $K=2E^{-13}\Phi^{10.688}$ (2)

7.2 Petrophysical analysis

There are three main lithofacies based on wireline log profiles: Sandstone, shaly sand and mudstone. Therefore, carbonate-cement sandstone was not defined clearly on the logs, although they are observed in several intervals of core samples. Sand will be defined by shaly sand model. A combination of density and neutron logs is useful in determining presence of hydrocarbons. Water saturations were derived by using the Dual Water Saturation model.

Porosity determination

Porosity is estimated by using density and neutron logs. Basically, single LLD log is also used for this purpose but it cannot be used in this case because of poor quality from 3286-3294 m (Fig. 18). The DT log is also not used for porosity calculation because it is affected by the over-pressured gas signature. The following formulas and were used to calculate porosity as in (3) and (4):

$$\phi_D = [(\rho_{ma}-\rho)/(\rho_{ma}-\rho_f)]-[Vsh\ (\rho_{ma}-\rho_{sh})/(\rho_{ma}-\rho_f)] \quad (3)$$

$$\phi_N = \phi - V_{sh}\,\phi_{Nsh} \quad (4)$$

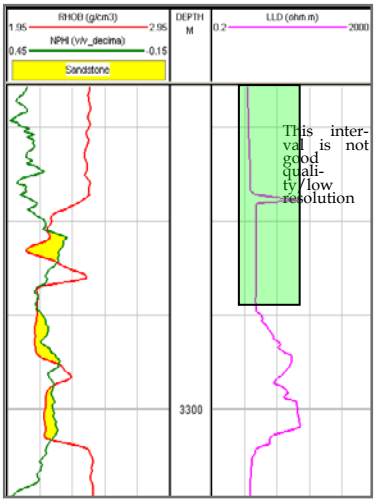

Fig. 18. LLD shows no good quality from 3286 to 3294m

The cross plot of density and neutron shows a gas effect over the sandstone intervals (Fig. 19).

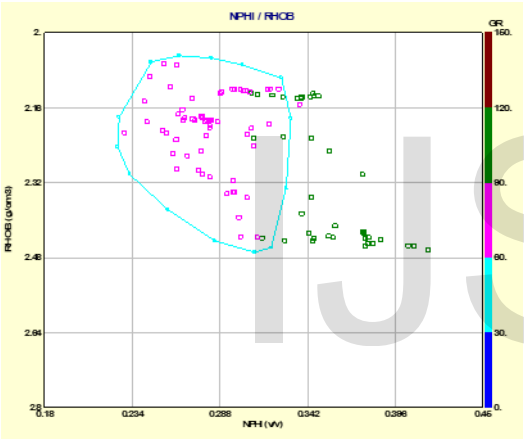

Fig. 19. Cross plot of Neutron and Density from 3286 to 3301 m

The derived-wireline effective porosity (PHIE) of sandstone lithofacies is generally consistent with the plug-derived porosity. PHIE of other lithofacies is slightly higher than plug-porosity. This may be because core porosity usually measures PHIE that excludes disconnected porosity and clay-bound water or that core porosity does not measured in fractures. Log-derived porosities measure total porosity. However, in shaly/silty sand lithofacies, the effective porosity is slightly smaller than the plug porosities. It is possibly due to the presence of siderite and ferrous dolomite cause in the density and resistivity values to be greater than normal grain density. Another reason is that lamination and fine sand sedimentary structures grain density and fine sand sedimentary structures with clay could not be recognized on gamma log, hence effective porosity and permeability could not be reliably estimated. Thus, it needs to be recalculated as effective porosity uses plug porosity. PHIE and core porosity of sandstone and shaly sand are shown in Fig. 20 [7].

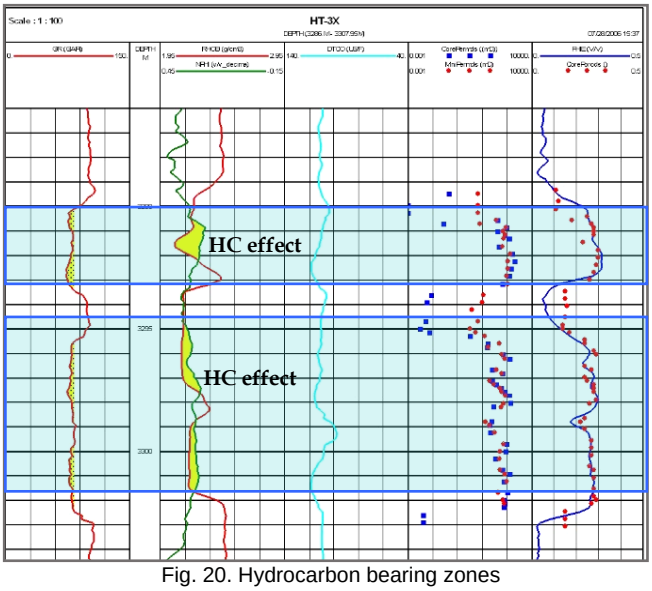

Fig. 20. Hydrocarbon bearing zones

The equations (5) and (6) present the relationship between PHIE and core porosity that can be applied for non-cored intervals in term of derived-permeability (Fig. 21).

Sand lithofacies: ϕ = -0.086811+ 1.32707*core (5)

Shaly sand lithofacies: ϕ = -0.673277-3.98144*core por (6)

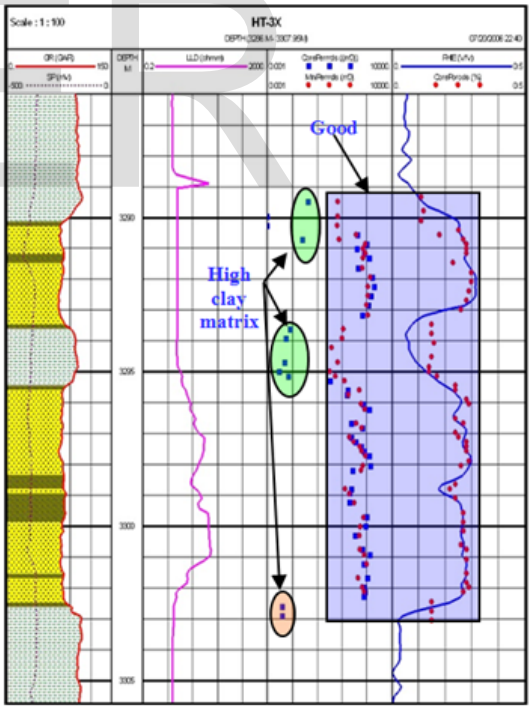

Fig. 21. Consistence of PHIE & Core porosity, mini-permeability & Core permeability relationships

Permeability derived from wireline data

Wireline-derived permeability of each lithofacies can be estimated from the porosity-permeability relationship (Fig. 22). In this case, a simple equation was selected for this calculation with sandstones facies with GR <83 API as in (7):

$Log_{10}K$ = -2.873489+19.27377*core por (7)

Porosity and Permeability relationship

Core porosity and core permeability Fig. 23 plotted to show the relationship between them for sandstone and shaly sand lithofacies. The equations (8) and (9) were applied to generate a static reservoir model based on the porosity and permeability relationships of the two lithofacies as follows:

Sandstone lithofacies:

Log K=-2.873489+19.27377*core por (8)

Shaly sand lithofacies:

Log K=-6.471788+30.27202*core por (9)

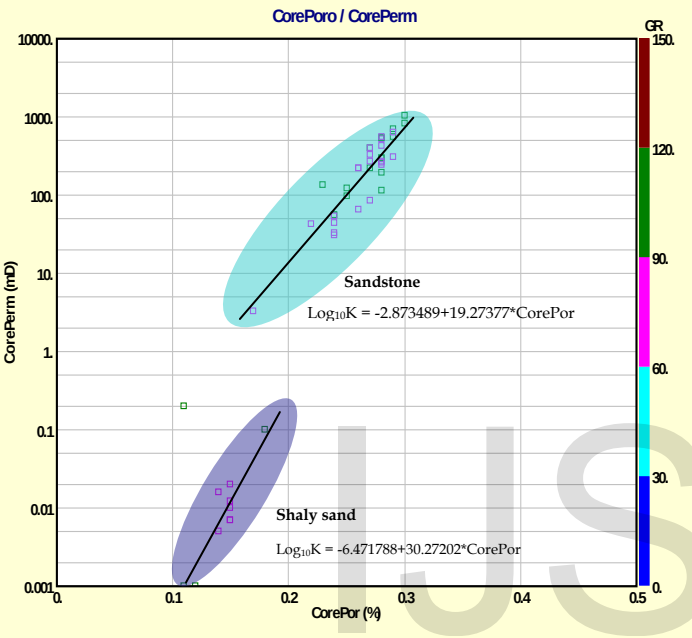

Fig. 22. Cross plot of core porosity and core permeability, 3286-3301m

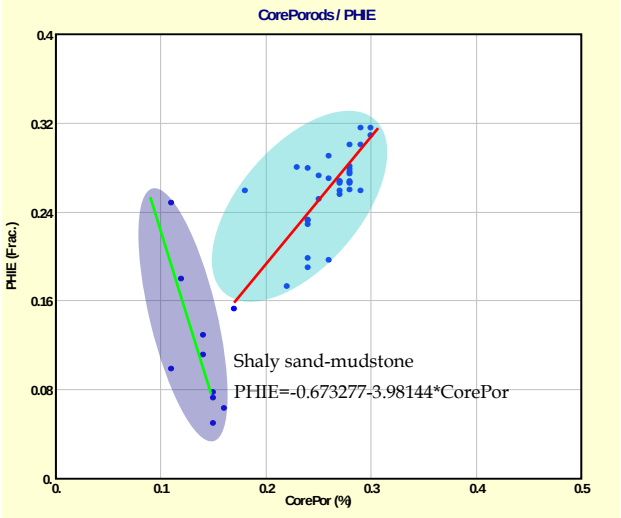

Fig. 23. Cross plot of core porosity and wireline porosity, 3286-3301m

8 Conclusion

Core material and wireline log of the HT-3X well have been used to produce a systemetic sedimentological interpretation. These logs suggest that very fine to fine-grained, mud/sand-rich sediments are the results of relatively high-density turbidity currents with longer transport route from the sediment source to the basin and a resulting better separate of sand and mud. Sediment deposition occurred within a submarine fan setting with facies ranging from Tb to Te divisions of Bouma sequences.

The well includes mainly lithofacies associations such as clean, massive, laminated sandstones with high porosity and permeability, indicative of good Miocene reservoirs.

Acknowledgment

The data in this paper has been supported by BP Vietnam Statoil and Prof. John K. Warren and Prof. Joshep J. Lambias of University Brunei Darussalam and Vietnam Petroleum Institute.

References

[1] BP, report 1999, Hai Thach Field reserve.

[2] J. lambias and J. Warren, 2005, Reservoir characterisation (Lecture style for Master program in Brunei).

[3] C. L. Dinwiddie, I. F. J. Molz and J. W. Castle, 2003, A new small drill hole minipermeameter probe for in situ permeability measurement: Fluid mechanics and geometrical factors: Water Resources Research, v. 39, pp. SBH21-SBH213.

[4] A. H. Bouma, 2000, Fine-grained, mud-rich turbidite systems: model and comparison with coarse-grained sand-rich systems, in Bouma, A. H. & C. G. Stone, eds-, Fine-grained turbidite systems, AAPG Memoir 72/SEPM special publication 68, pp. 9-20.

[5] J. Warren, 2005, Introduction to wireline logs (Lecture style of Master program in Brunei)

[6] R. M. Bateman, C. E. Konen, 1977, The log analyst and the programmable pocket calculator, part II-Cross-plot, porosity and water saturation: Log analyst, Vol. 18, No. 6, pp. 3-11

[7] V. T. H. Quan, 2006. Depositional characterisation of Upper Miocene, wells HT-2X and HT-3X, Hai Thach field, Nam Con Son basin, offshore Southern Vietnam (Master thesis style in University of Brunei Darrusalam).